Physica D 38 (1989) 322–329
North-Holland, Amsterdam

NEW RESULTS ON THE FRACTAL AND MULTIFRACTAL STRUCTURE OF THE LARGE SCHMIDT NUMBER PASSIVE SCALARS IN FULLY TURBULENT FLOWS

K.R. SREENIVASAN and Rahul R. PRASAD
Mason Laboratory, Yale University, New Haven, CT 06520, USA

By measuring concentration fluctuations of a dye with very fine spatial and temporal resolution in typical unconfined turbulent water flows, we obtain the fractal dimension characteristic of the scalar interface in the range between Kolmogorov and Batchelor scales. We use one-dimensional intersection methods and invoke Taylor's hypothesis, but both of them are amply justified. We obtain a theoretical estimate for the fractal dimension by modifying our earlier arguments for finite (though large) Schmidt number effects. Finally, the multifractal characteristics of the scalar dissipation rate in the same scale range are also presented.

1. Introduction

A trace of dye or smoke, or a suspension of the fine particles of a metal, is considered a passive scalar if it does not affect the dynamics of the flow into which it is introduced. The behavior of passive scalars in turbulent flows is interesting in its own right, and the understanding of its mixing is practically useful in several contexts including combustion; since their evolution is determined by the velocity field, passive scalars can be studied profitably as a diagnostic even if the primary focus is on the dynamics of turbulent motion.

It is now well known [1] that an unbounded turbulent flow such as a jet develops at high Reynolds numbers "fronts" across which vorticity changes are rather sharp on scales larger than the characteristic thickness of the fronts. Such a front, called the vorticity interface, retains its sharpness in spite of the natural tendency of vorticity to diffuse: The nonlinear stretching inherent in the quadratic terms of the fluid equations provides the balancing action. A passive scalar introduced in fully turbulent flows gets dispersed by turbulence, and itself displays a sharp front across which the scalar concentration shows similar large jumps. In analogy with the vorticity interface, this front is called the scalar interface. This is the object of our interest here.

The scalar interface is a complex surface residing in three-dimensional physical space (see fig. 1); it is quite convoluted over a range of scales which are statistically self-similar. At high enough Reynolds numbers, there is a large separation between the largest and smallest scales on which the interface appears convoluted, and this allows the use of fractals [2] in characterizing the interface [3–6]. Unlike a mathematical fractal, the scale-similar regime of the interface is bounded on both sides by physical effects; the upper cutoff occurs at a (fraction of) the integral scale of motion, this being comparable to (but distinctly less than) the gross size of the flow such as the width of the jet, whereas the inner cutoff occurs at a scale where the effects of scalar diffusivity are felt directly. When the Schmidt number σ (that is the ratio of the fluid viscosity to scalar diffusivity) is unity, this scale is the Kolmogorov scale η equal to the smallest dynamical scale of the vorticity interface. If σ is much smaller than unity (as in the steller atmosphere) the smallest scalar scale is the so-called Batchelor scale $\eta_b = \eta = \sigma^{-1/2}$ [7]. This is typically the case of a dye mixed in water; the molecular structure of water is such that the colliding dye molecules transfer mo-

Essays in honour of Benoit B. Mandelbrot
Fractals in Physics – A. Aharony and J. Feder (editors)

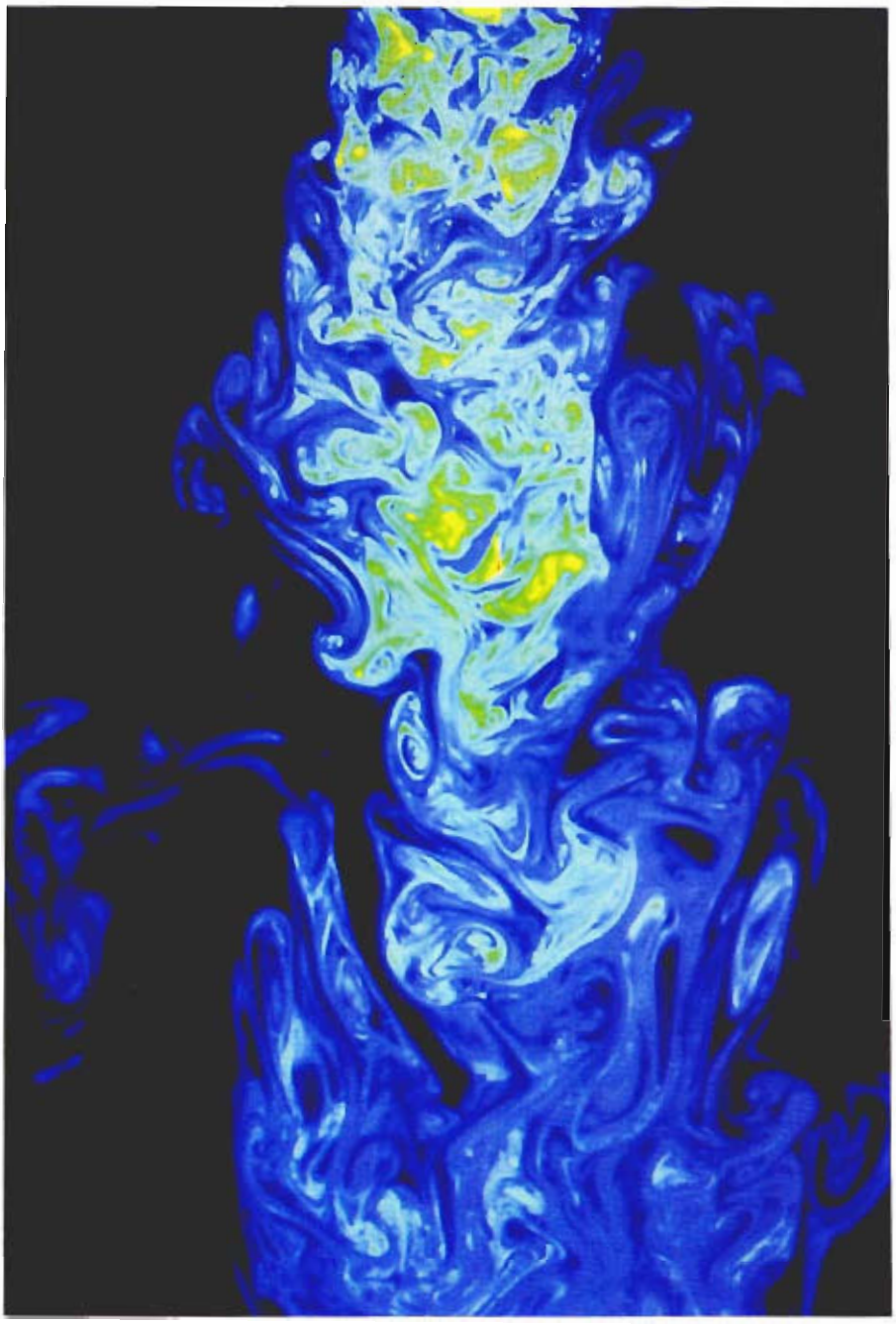

Fig. 1. To demonstrate the complexity of the scalar interface, we show a two-dimensional section of a turbulent jet at a nozzle Reynolds number of about 4000, obtained by the laser-induced fluorescence technique. Only scales coarser than the Kolmogorov scale are resolved. The digital camera used to obtain this image has an array size of about 1300×1000 pixels. The region imaged extends from 8 to 24 diameters downstream of the nozzle. A Nd YAG laser beam shaped into a sheet of 200–250 μm thickness using suitable lenses was directed into a water tank into which the nozzle fluid containing small amounts of a fluorescing dye was emerging in the form of a jet. The laser had a power density of 2×10^7 J s^{-1} per pulse and a pulse duration of about 10 ns. The flow is thus frozen in this picture to an excellent approximation.

mentum much more efficiently than their own mass.

In our previous work, we used a dye mixed in water flows and resolved all scales above η, which, in a typical experiment, was around 200 μm. The Schmidt number was [8] of the order of 2000, yielding a Batchelor scale of about 4–5 μm. It is easy to argue [7,9] that a different scaling regime should exist between η_b and η. It is therefore interesting to resolve these scales and determine their scaling properties. This is the first purpose of the paper.

In the flow interior far from the boundary, the scalar concentration fluctuates in both space and time. The square of the gradient of these fluctuations represents (to within a constant) the rate at which the fluctuation intensity is being smeared by molecular diffusivity. This quantity is called the scalar dissipation rate, χ. We have shown earlier [10] that χ possesses a multifractal distribution – again with the qualification that cutoffs are present. As before, the spatial resolution was limited to Kolmogorov scale. Our second purpose is to determine the multifractal scaling properties of χ between η_b and η.

2. The method

As remarked earlier, the scalar interface is a fractal-like surface embedded in three-dimensional space, and we want to determine its fractal dimension. Following [3,4], we shall use box-counting methods which involve covering the volume by three-dimensional boxes of varying sizes, and counting the number of boxes containing the interface. The exponent characterizing the variation of this number with respect to the box size will give the fractal (i.e. box) dimension of the interface. The current limitations of instrumentation technology permit this direct method to be used only as long as the volume to be scanned is not too large and the resolution required is not too demanding. Such measurements have been made by Prasad and Sreenivasan [6], who resolved a volume of the order of $25\eta \times 300\eta \times 300\eta$ with resolution of between 2η and 3η. In general, fluid dynamical constraints are much stronger, and the more feasible way of obtaining the fractal dimension is to use the method of intersections. Here, one intersects the interface by a thin plane or a line – thin meaning that the finest scales of interest are resolved – and obtaining the fractal dimension of the intersections. The fractal dimension of the surface itself is then obtained by the so-called additive law for co-dimensions (see ref. [2] and references cited here), according to which the intersection by a plane results in a set whose dimension is one less than the dimension of the original set; when intersected by a line, the fractal dimension is two less than the dimension of the original set.

The requirement that the Batchelor scale be resolved allows only trivial extents of the flow to be mapped even in two-dimensional intersections; one therefore has to resort only to one-dimensional intersections. These can be obtained rather easily by invoking Taylor's frozen flow hypothesis according to which turbulence convects undistorted with the mean motion. This is reasonably accurate, especially for small scales of motion, if the mean convection velocity of the flow is large compared to its fluctuations. The relevant ratio is about 60 for the wake behind a cylinder and is large enough, but is only of the order of 4 for jets. It turns out that *geometric* aspects such as the fractal dimension are quite insensitive to details such as Taylor's hypothesis; in ref. [3], we showed that even for jets the fractal dimension results can be obtained quite accurately in this way. On the other hand, *dynamical* aspects such as the spectral distribution of the scalar variance are much more sensitive to Taylor's hypothesis [11].

3. The flows and the measurement technique

A turbulent wake behind a circular cylinder was produced by lowering a tank of water past a rigidly mounted cylinder. The cylinder was 1 cm in diameter and had an aspect ratio of 58. The tank was lowered at a constant speed of 15 cm/s by means of a hydraulic lift. The fluorescent dye (sodium fluorescein) that seeped into the wake from a narrow chan-

nel cut along the length of the cylinder – either at the front or the back stagnation regions – was mixed by the turbulence in the wake. The flow Reynolds number of 1500 (based on the cylinder diameter and the free stream relative speed) is moderate. During data acquisition, the position of measurement varied between 60 and 70 diameters behind the cylinder. The Kolmogorov and Batchelor scales were estimated to be about 160 and 4 μm, respectively.

A jet was produced by allowing water to flow from a settling chamber through a nozzle of circular cross-section (diameter 1.2 cm) into a tank of still water at a constant speed of about 35 cm/s. The nozzle was contoured according a fifth-order polynomial to have zero slopes and curvature at the entrance and the exit. The contraction ratio was about 10. The jet Reynolds number based on nozzle diameter and exit velocity was about 4000. During data acquisition, the position of measurement varied between 20 and 37 nozzle diameters downstream. The estimated Kolmogorov and Batchelor scales in the measurement region are about 200 and 5 μm, respectively.

The optical setup is shown in fig. 2. By various combinations of lenses described in the caption, the beam is focused to a spot of about 4 μm at the desired location in the flow. Concentration fluctuations are detected as fluctuations in fluorescence intensity, the two being in linear proportion to each other. The optical signal from the photomultiplier tube is passed through a current amplifier before being digitized by the 12-bit A/D converter on the MASSCOMP 5000 computer. The digitizing frequency is set at 320 kHz, which is well below the limiting digitization rate of 1 MHz of the A/D converter. The photomultiplier tube is quoted by the manufacturer as having good frequency response up to 50 MHz. So the temporal response of the instrumentation is believed to be much better than is required for present purposes.

From the highly resolved concentration fluctuation signal c, we obtain the fractal dimension of the interface as well as the multifractal aspects of χ. We have demonstrated in ref. [11] that the signal possesses the expected classical properties, for example the correct power law behaviors.

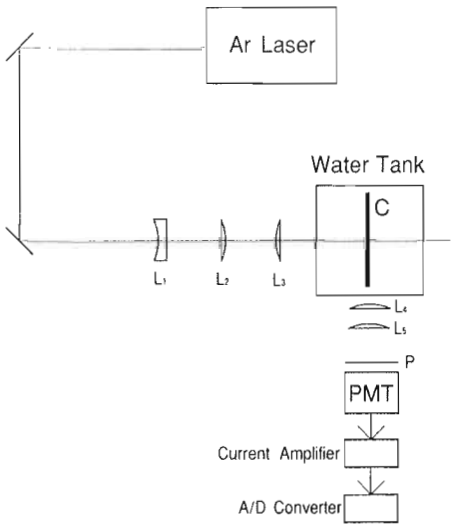

Fig. 2. Schematic of the optical setup. Shown is the orientation of the cylinder (C), whose wake is the flow of interest here. A 5 mm diameter light beam from the continuous argon laser (power output about 7 W) is first expanded into a thicker beam of 60 mm diameter by the combination of spherical lenses L_1 (focal length 25 mm) and L_2 (focal length 300 mm), and then focused to a spot of 5.5 μm diameter by means of a convex lens L_3 of focal length 500 mm. The optical signal is collected by a photomultiplier tube (PMT). In the optical path upstream of the photomultiplier tube is a combination of lenses L_4 and L_5 (focal lengths 400 and 1000 mm, respectively) that give an image enlargement by a factor of 2.5. This combination enlarges the 5.5 μm focal spot in the flow to a size of about 13 μm. Ahead of the photomultiplier tube, a 10 μm diameter pinhole (P) is located. This effectively reduces the size of the spot imaged onto the phototube to 4 μm, this being the spatial resolution of measurement.

4. Results

Fig. 3 shows a typical plot of the logarithm of the number of boxes containing the intersection points of the interface as a function of box size. There are two distinct power law regimes, one of which occurs (roughly) between η_b and η, and the other to the right of η. As expected from earlier measurements [3–6], the negative slope in the latter region is around 0.36 – giving a fractal dimension of 2.36. (The scatter in that region is relatively large because the limited duration of the signal did not contain too many inter-

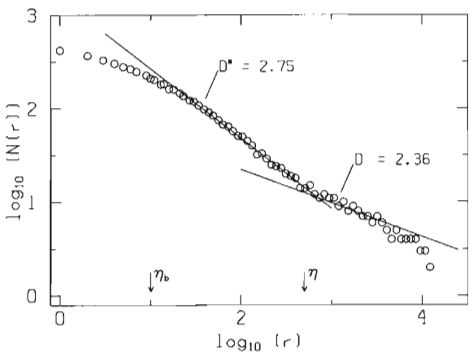

Fig. 3. A typical log–log plot of the number $N(r)$ of length elements or "boxes" of size r containing the interface versus the box size r. The flow is the wake of a circular cylinder. The negative slopes of the straight parts give, in the respective scaling regime, the fractal dimensions of one-dimensional intersections of the boundary. The dimension, corresponding to the slope of the line drawn in the region between η and L, is about 2.36. That in the range between η and η_b is about 2.75.

sections comparable to the bigger boxes.) The region between η_b and η has a slope of about -0.75, giving the fractal dimension to be about 2.75. The average slope from several realizations is 2.7 ± 0.03. Data from jets confirm this conclusion.

This is our first main result, and we should like to explain it. This is done by considering the dye mixing at infinitely large Schmidt numbers [9], and then providing corrections for the finite (but large) Schmidt numbers.

The basic idea is that the properties of the scalar interface and the mixing of the scalar with the ambient fluid are related. Since the amount of mixing is governed by large eddies in the flow, the actual process of mixing (by which we mean molecular mixing) is accomplished by diffusion across the surface whose geometry is determined by the requirement that it accomplish the exact amount of mixing set by the large scales. Thus, even though the process is initiated by large scales, one can legitimately concentrate on the diffusion end. This approach has a much better likelihood of yielding results of some "universality", simply because the small-scale features of the flow are, to a first approximation, independent of configurational aspects of the flow. The fractal dimension of the interface is but one example. This approach neither minimizes the role of large eddies nor resorts to gradient transport models usually discredited in turbulence theory.

Motivated by this thinking, Sreenivasan et al. [9] concentrated on the last stages of the mixing process by working with diffusion across the fractal-like interface. They proceeded from Fick's law of diffusion, which can be expected to hold accurately in spite of the high degree of convolutedness of the surface (because the scales of convolutions are significantly larger than the molecular mean free path), and showed that the flux of the scalar is given by

$$\beta \, \mathrm{Re}^{3(D-7/3)/4} \sigma^{(D^*-3)/2} , \tag{1}$$

where β (which in ref. [9] has been written down explicitly) consists only of quantities depending on the large-scale features of the flow and are independent of Reynolds number. D is the fractal dimension in the scale range between η and L, and D^* in the range between η and η_b. Re is the flow Reynolds number given by $u'L/\nu$; u' is the root-mean-square fluctuation velocity and ν is the kinematic viscosity of the fluid.

One can then invoke [9] the so-called Reynolds number similarity, which is merely a statement of the observed fact that all fluxes (mass, momentum, energy) must be independent of Reynolds number in fully turbulent flows. According to (1), Reynolds number similarity requires that

$$D = 7/3 , \tag{2}$$

in rough agreement with experiments [3–7,9]. Multifractal corrections [9,12] change this value slightly to $D = 2.36$, bringing it identically equal to the measured average [4,9].

Similarly, Schmidt number similarity requires that

$$D^* = 3 . \tag{3}$$

This means that convolutions of the interface on scales between η_b and η are space-filling. The physical picture corresponding to this situation was described in ref. [9].

This last result, of specific interest here, gets mod-

ified when the Schmidt number remains finite (though large). To quantify the effect, we recapitulate that an essential argument used in ref. [9] is that the concentration gradient across the interface is of the order of c'/η_b, where c' is the root-mean-square of the concentration fluctuation c – a large-scale feature. It turns out [7] that the time taken by the scalar to diffuse down to the Batchelor scale increases logarithmically with the Schmidt number. There is also a corresponding pile up of fluctuation intensity in the scalar patches as the straining by the velocity field continues unabated. The effective concentration gradient is then given by $c'(\ln\sqrt{\sigma})/\eta_b$, and the expression (1) for the flux gets multiplied by the factor $\ln\sqrt{\sigma}$. It is then easy to show that the Schmidt number similarity requires that

$$D^* = 3 - 2\ln(\ln\sqrt{\sigma})/\ln\sigma\,. \tag{4}$$

In the limit of infinite Schmidt numbers (4) reduces to (3). For a Schmidt number of 1930, as for the fluorescing dye [8], (4) yields the result that $D^* = 2.65$, quite close to the measured value of 2.7.

We reiterate that the present arguments hold in circumstances where the amount of mixing is determined by the large scale, and the surface adjusts itself accordingly. For large eddies to be the controlling factor at infinitely large Schmidt numbers, it is necessary that the Reynolds number must be correspondingly large, the precise condition being that $(\ln\sigma)/\mathrm{Re}^{1/2} \ll 1$. As expected on physical grounds, this condition never lets the characteristic gradient across the interface exceed $\Delta c/\eta_b$, where Δc is the maximum concentration difference in the flow.

The result that the interface has space-filling characteristics in the Batchelor regime (scale sizes between η_b and η) suggests that other aspects of the scalar in this scaling regime might also be space-filling in the limit of infinite σ. In particular, the scalar dissipation rate χ might be space-filling also. If so, all the generalized dimensions [13] will all be unity, and the multifractal spectrum, or the $f(\alpha)$ curve [14], trivially reduces to the point (3, 3) in three dimensions and to the point (1, 1) in one-dimensional intersections. Finite Schmidt number effects may alter this result, and it would therefore be useful to obtain from experiment the generalized dimensions. We follow the procedure described in ref. [12].

The generalized dimensions D_q are obtained by dividing a record of scalar dissipation into smaller boxes of size r, and identifying power laws of the type

$$\sum (X_r)^q \sim r^{(q-1)D_q}\,, \tag{5}$$

where X_r is the total dissipation over a box of size r, and the sum is taken over all boxes of size r; q is any real number. It is clear that if q is positive and large, only the large intensity regions will be picked by the summation in (5) while the least intense regions correspond to large negative q's. According to (5), if log–log plots of $[\sum (X_r)^q]^{1/(q-1)}$ versus r present linear regions within the scaling range $\eta_b < r < \eta$, the slopes correspond to the D_q's.

The D_q and the $f(\alpha)$ curves for one-dimensional sections of the dissipation of turbulent kinetic energy were measured in ref. [12] and shown to be universal features of fully developed turbulence. Similar measurements in refs. [6,10] for the scalar dissipation were made from two- and three-dimensional images in the scale range between η and L. Since we have measured – as already explained, by the application of Taylor's hypothesis – one component of χ with resolution of the order of the Batchelor scale, our purpose here is to measure the D_q curve in the Batchelor regime. We note the earlier result [6,10] that the multifractal properties of a single component of χ are the same as those of χ itself, and that Taylor's hypothesis is adequate for the purpose.

Typical log–log plots of $[\sum (X_r)^q]^{1/(q-1)}$ versus r are shown in fig. 4 for some representative q values. For clarity and convenience, only the scaling in the Batchelor regime is shown. The straight line regions yielding the D_q's are quite unambiguous. The $f(\alpha)$ curve can be computed from Legendre transforms, but these results are not presented here.

Fig. 5 shows the curve of D_q versus q for the Batchelor regime. We have invoked the additive law and added 2 to the results obtained from one-dimensional intersections. As expected, all the generalized dimensions are quite close to the box dimension D_0

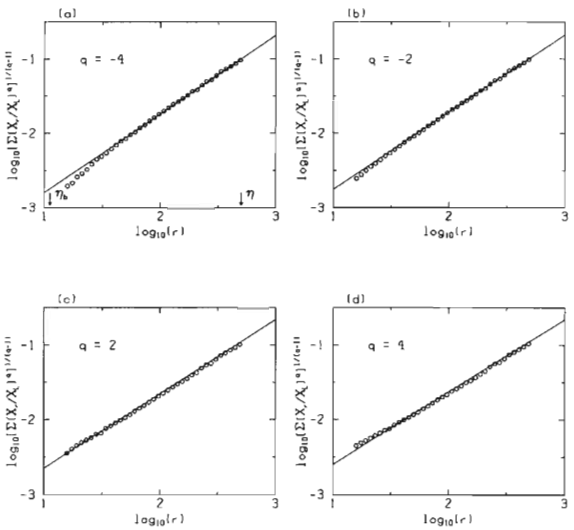

Fig. 4. Typical log–log plots of $[\sum(X_r)^q]^{1/(q-1)}$ versus r from the dissipation field of the jet for four different values of q; (a) $q=-4$, (b) -2, (c) 2, (d) 4. Power law regions are seen for each q, extending approximately between η and η_b.

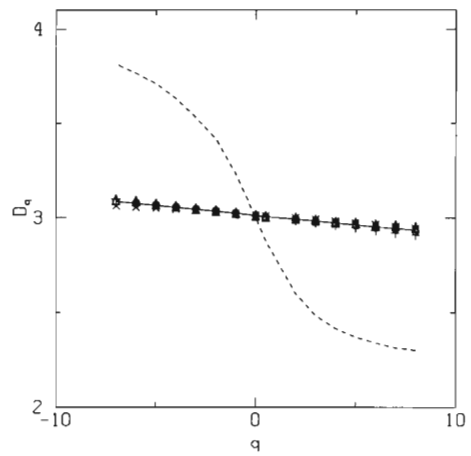

Fig. 5. The generalized dimensions for the scalar dissipation. Different symbols correspond to different realizations, and the solid line represents the mean. The dashed line shows results for the range between η and L [10]. The present results for the range between η and η_b show that all the D_q's are much closer to D_0. The expectation is that they will identically be equal to D_0 in the limit $\sigma=\infty$. The additive law has been used in presenting the results.

of the support. Fig. 5 also compares the present results to those previously obtained [10] in the scaling range between η and L. Unlike the interface dimension, it is difficult to interpret the generalized dimensions physically and obtain theoretical estimates.

5. Summary of results

Two distinct scaling regimes, and therefore two distinct fractal dimensions, exist for the scalar interface in the high Schmidt number case. The two separate scaling regimes reflect the fact that the dominant physical effects are different in the two regimes. For example, the Kolmogorov scale plays no role in the Batchelor regime except that it acts as a cutoff scale analogous to the integral length scale in the regime between η and L. In the scaling range between L and η, the fractal dimension is 2.36 ± 0.05; this result also holds for the vorticity interface [3]. The Batchelor regime possesses another fractal dimension, which is 3 for infinitely large Schmidt numbers – assuming, of course, that mixing is still controlled by large eddies. As remarked already, the condition for the latter is that the square root of the Reynolds number must be large compared to the logarithm of the Schmidt number. Unlike finite Reynolds number effects, finite Schmidt number corrections are significant; even if σ is about 2000, both experiments and a simple theory of mixing show that the fractal dimension is only as high as 2.7.

Generalized dimensions of χ in the flow interior are quite close to D_0 in the Batchelor regime. Among other things, it means that the intermittency corrections in that regime are quite negligible. If we extrapolate our experience with finite Schmidt number corrections for the interface dimension, we may speculate that all the D_q's for $\sigma=\infty$ will equal D_0, and that the intermittency corrections are identically zero.

By his own work and through his influence on others, Benoit Mandelbrot has had a vigorous and long-lasting influence in charting frontiers of science in

many areas including turbulence. This paper is a modest expression of our intellectual indebtedness to him. It is a pleasure to dedicate it to Benoit on the occasion of his 65th birthday. The work was financially supported by DARPA (URI) and AFOSR.

References

[1] S. Corrsin and A.L. Kistler, NACA Rep. (1955) 1244.
[2] B.B. Mandelbrot, The Fractal Geometry of Nature (Freeman, San Francisco, 1982).
[3] K.R. Sreenivasan and C. Meneveau, J. Fluid Mech. 173 (1986) 357.
[4] K.R. Sreenivasan, R.R. Prasad, C. Meneveau and R. Ramshankar, J. Pure Applied Geophys. 131 (1989) 297.
[5] R.R. Prasad and K.R. Sreenivasan, Exp. Fluids 7 (1989) 259.
[6] R.R. Prasad and K.R. Sreenivasan, in: Proceedings of Turbulent Shear Flows (Seventh Symposium), Stanford (August 1989), also submitted to J. Fluid Mech.
[7] G.K. Batchelor, J. Fluid Mech. 5 (1959) 113.
[8] B.R. Ware et al., in: Measurement of Suspended Particles by Quasi-elastic Light Scattering, B.E. Dahneke, ed. (Wiley, New York, 1983), p. 435.
[9] K.R. Sreenivasan, C. Meneveau and R. Ramshankar, Proc. Roy. Soc. (London) A 421 (1989) 79.
[10] R.R. Prasad, C. Meneveau and K.R. Sreenivasan, Phys. Rev. Lett. 61 (1988) 74.
[11] K.R. Sreenivasan and R.R. Prasad, in preparation.
[12] C. Meneveau and K.R. Sreenivasan, Nucl. Phys. B. Proc. Suppl. 2 (1987) 49.
[13] H.G.E. Hentschel and I. Procaccia, Physica D 8 (1983) 435.
[14] T.C. Halsey, M.H. Jensen, L.P. Kadanoff, I. Procaccia and B.I. Shraiman, Phys. Rev. A 33 (1986) 1141.